Available online at www.sciencedirect.com
SCIENCE DIRECT®
Agricultural and Forest Meteorology 125 (2004) 187–205
AGRICULTURAL AND FOREST METEOROLOGY
www.elsevier.com/locate/agrformet

# Airflows and turbulent flux measurements in mountainous terrain Part 2: Mesoscale effects

Andrew A. Turnipseed [a,b,*], Dean E. Anderson [c], Sean Burns [a], Peter D. Blanken [d], Russell K. Monson [a,e]

[a] *Department of Environmental, Population and Organismic Biology, University of Colorado, Boulder, CO 80309, USA*
[b] *Atmospheric Chemistry Division, National Center for Atmospheric Research, 1850 Table Mesa Dr., Boulder, CO 80305, USA*
[c] *US Geological Survey, Water Resources Division, Denver Federal Center, Lakewood, CO 80225, USA*
[d] *Department of Geography, University of Colorado, Boulder, CO 80309, USA*
[e] *Cooperative Institute for Research in Environmental Sciences (CIRES), University of Colorado, Boulder, CO 80309, USA*

Received 12 September 2003; received in revised form 2 April 2004; accepted 27 April 2004

**Abstract**

The location of the Niwot Ridge Ameriflux site within the rocky mountains subjects it to airflows which are common in mountainous terrain. In this study, we examine the effects of some of these mesoscale features on local turbulent flux measurements; most notably, the formation of valley/mountain flows and mountain lee-side waves. The valley/mountain flows created local non-stationarities in the wind flow caused by the passage of a lee-side convergence zone (LCZ) in which upslope and downslope flows met in the vicinity of the measurement tower. During June–August, 2001, possible lee-side convergences were flagged for ∼26% of all half-hour daytime flux measurement periods. However, there was no apparent loss of flux during these periods. On some relatively stable, summer nights, turbulence (designated via $\sigma_w$), and scalar fluctuations (temperature and $CO_2$, for example) exhibited periodicities that appeared congruent with passage of low frequency gravity waves ($\tau \sim 20$ min). Spectral peaks at 0.0008 Hz (20 min) in both vertical velocity and scalar spectra were observed and indicated that 25–50% of the total scalar covariances were accounted for by the low frequency waves. During some periods of strong westerly winds (predominantly in winter), large mountain gravity waves were observed to form. Typically, the flux tower resided within a region of downslope "shooting flow", which created high turbulence, but had no detrimental effect on local flux measurements based on valid turbulence statistics and nearly complete energy budget closure. Periodically, we found evidence for re-circulating, rotor winds in the simultaneous time series of wind data from the Ameriflux tower site and a second meteorological site situated 8 km upslope and to the West. Only 14% of the half-hour time periods that we examined for a 4 month period in the winter of 2000–2001 indicated the possible existence of rotor winds. On average, energy budget closure was ∼20% less during periods with rotor occurrence compared to those without.

Results from this study demonstrate that the potential exists for relatively rare, yet significant influences of mesoscale wind flow patterns on the local half-hour flux measurements at this site. Occurrence of these events could be detected through examination of normal turbulence statistical parameters.


*Keywords:* Ameriflux; Complex terrain; Mountain circulations; Rotor winds; Lee-side convergence zone; Mountain waves; Stationarity; Energy balance

* Corresponding author. Tel.: +1 303 497 1448.
*E-mail address:* turnip@ucar.edu (A.A. Turnipseed).

0168-1923/$ – see front matter © 2004 Elsevier B.V. All rights reserved.
doi:10.1016/j.agrformet.2004.04.007

## 1. Introduction

In recent years, a number of tower-based flux networks have been established to understand controls over mass and energy fluxes between the biosphere and atmosphere (Aubinet et al., 2000; Baldocchi et al., 2001). Eddy covariance (EC) measurements are the cornerstone for these networks, as they provide a direct measure of the flux and allow nearly continuous coverage over time. However, a basic assumption of the EC method is that the flux measured at one point is representative of the surrounding, underlying surface (Kaimal and Finnigan, 1994; Foken and Wichura, 1996; Massman and Lee, 2002). This assumes spatial homogeneity and no net flow convergence or divergence. These assumptions are rarely met within natural plant communities, particularly in non-simple terrain.

The EC method has rarely been applied in mountainous ecosystems due to concerns that in complex terrain, variations in vegetation, near-surface groundwater hydrology, and airflow patterns would lead to violations of the basic assumptions mentioned above. However, recent regional modeling analyses have indicated the importance of biogeochemical cycling in mountainous ecosystems (Schimel et al., 2002). This study predicted that during periods of extended drought (e.g., decadal-scale drought during the 1980's), carbon sequestration by Pacific coastal forests in the US would be markedly suppressed, and regional foci of high carbon uptake occurred in continental montane and subalpine forests. In terms of regional hydrology, the importance of mountainous ecosystems has long been recognized (Barry, 1993), as mountain regions supply more than half the world's freshwater (Ives et al., 1997). Considering the importance of mountain ecosystems in the linked carbon–hydrological cycles and our dependence on the EC method in their measurement, there is clearly a need to better understand limitations to the EC method in these environments, and possible ways to improve it use in these ecosystems.

We have been measuring EC fluxes of heat, momentum, $H_2O$ and $CO_2$ at the Niwot Ridge Ameriflux site since November 1998. The site lies on the Eastern side of the Rocky Mountains in complex terrain. Using 2 years of data, energy budget closure at the site was nearly complete during periods characterized by high friction velocity ($u^* > 1.2\,\mathrm{m\,s^{-1}}$). On average, closure was similar to that reported for sites with more ideal, flat terrain (~84% closure, Turnipseed et al., 2002). An analysis of the canopy and local topography near the flux tower, and their effects on flux statistics, revealed no adverse effects on most daytime flux measurements. Nocturnal measurements with low friction velocity ($u^* < 0.3\,\mathrm{m\,s^{-1}}$) were complicated by the presence of downslope gravitational flows which were decoupled from above-canopy flows. The formation of these drainage flows likely led to substantial advective fluxes (Turnipseed et al., 2003).

Mountainous terrain surrounding the Niwot Ridge site can induce larger-scale meteorological phenomena that could affect local turbulent flux measurements. Previous investigators have surmised that large, mesoscale motions can influence local flux measurements (Sun et al., 1997, 1998; Desjardins et al., 1997; Panin et al., 1998; Mahrt, 1998), although there are few quantitative studies (Panin et al., 1998; Sakai et al., 2001; Finnigan et al., 2003). In this, the second part of the series, we present evidence of several large-scale flow characteristics that occur at the Niwot Ridge site due to interactions with the underlying terrain. These complex flow patterns include: (1) alternating upslope/downslope flows and (2) mountain gravity waves with concomitant rotor winds. We examined these large-scale flows features in an effort to determine how they affect local flux measurements (primarily energy and $CO_2$ fluxes) at the site.

## 2. Site description

Fig. 1 shows a regional digital elevation map of the front range of Colorado and includes the measurement site (located at 40° 1′ 58.4″N and 105° 32′ 47.0″W), the higher mountain peaks (approximately 8 km to the West of the site), and the beginning of the great plains about 25 km to the East. The Niwot Ridge Ameriflux site is situated on Arapahoe Moraine at an elevation of 3050 m. A detailed map showing the "local" site topography has been presented in Turnipseed et al. (2002, 2003). The predominant winds are from the West (Barry, 1973; Brazel and Brazel, 1983), flowing downslope. Summertime meteorology produces valley–mountain airflows, with thermally-induced, near-surface anabatic (upslope)

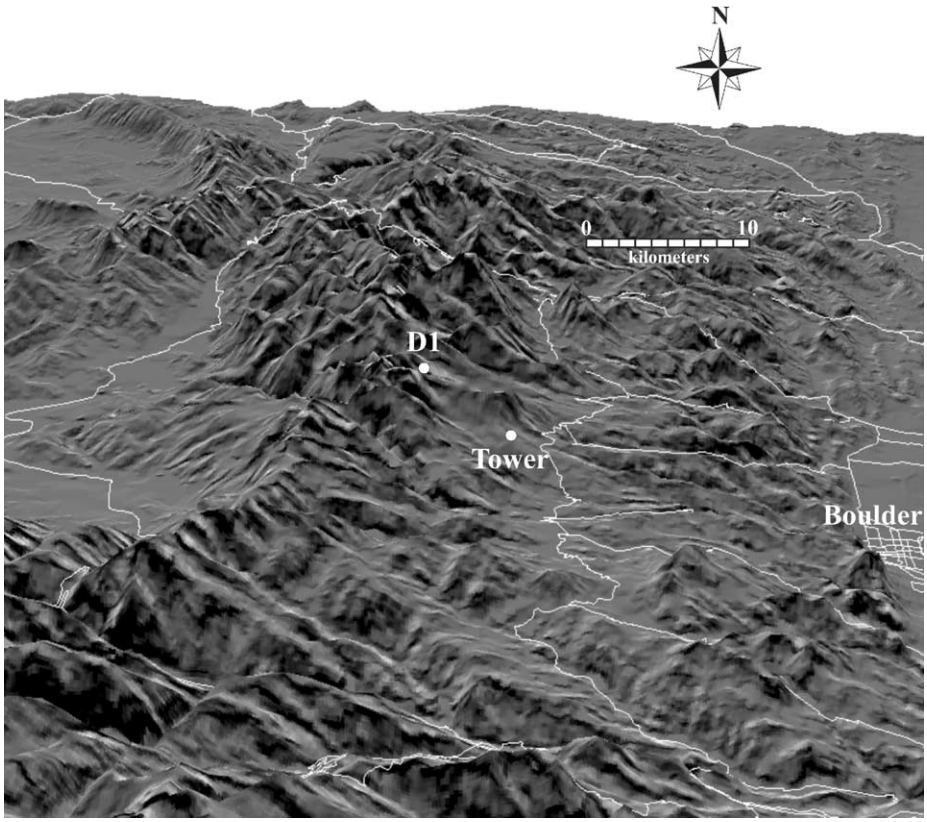


Fig. 1. Digital elevation map of the rocky mountain region near the Niwot Ridge Ameriflux site. Elevations are exaggerated by a factor of two relative to horizontal distances. The Ameriflux flux tower and the D1 meteorological station are each denoted by bullets.

winds from the East occurring on many afternoons (approximately one-third of the days), contrary to the higher, geostrophic westerly wind (Fig. 2a). Upslope flow also occurs with large synoptic storm systems passing to the South of the region, or upon the passage of cold fronts associated with the approach of high pressure region from the North. These events are often accompanied by precipitation. Nighttime flow is nearly always from the West, and is often katabatic (downslope drainage) flow.

Flux and meteorological measurements were made from a 26 m tall scaffolding tower. The tower is situated within a mixed coniferous forest of subalpine fir (*Abies lasiocarpa*), Engelmann spruce (*Picea engelmannii*) and lodgepole pine (*Pinus contorta*), in terrain gently sloping (5–7°) from West to East. The average canopy height ($h_c$) is 11.4 m with an average tree density of 4000 stems $ha^{-1}$, a leaf area index of 3.8–4.2 $m^2$, and a canopy gap fraction of 17%. Other details of the study site can be found in Turnipseed et al. (2002, 2003), and Monson et al. (2002). Additional meteorological data were taken above the tree line (elevation of 3740 m) at the D1 meteorological station (see Fig. 1). This site lies near the Continental Divide approximately 8 km west of the primary flux tower.

## 3. Instrumentation and methods

Vertical profiles of wind speed and direction were measured by a combination of sonic anemometry and helicoid propeller anemometers ($z = 1$, 3, 6, 9, 16, 21.5 and 26 m). Within the canopy, where wind speeds were lower and direction highly variable, only sonic anemometry was used; either with

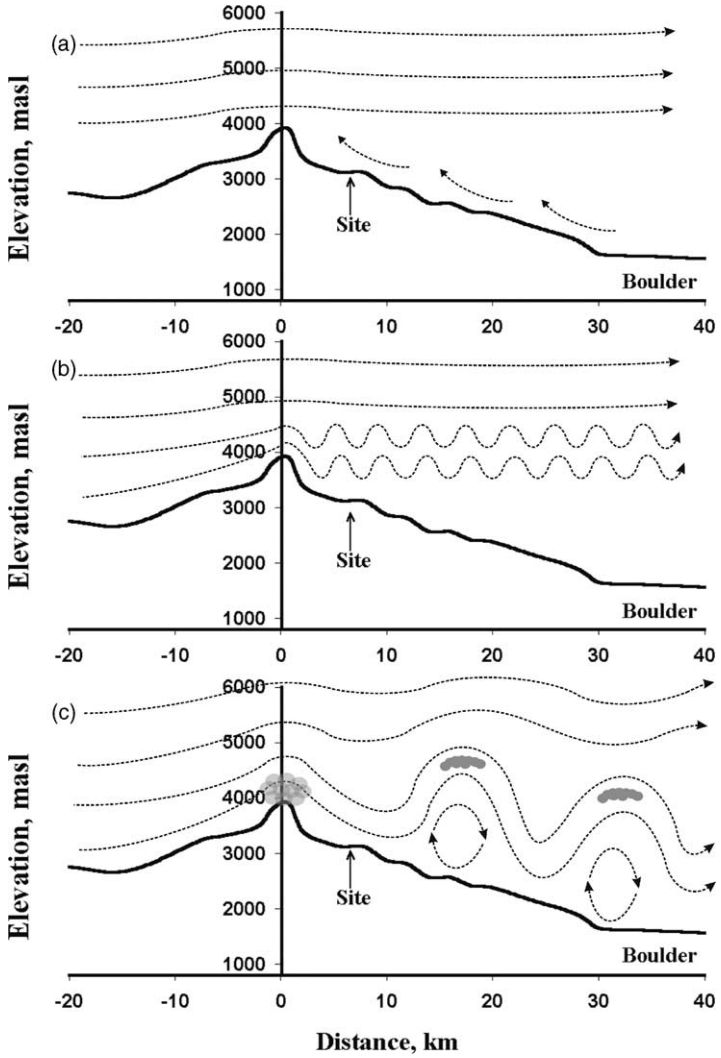


Fig. 2. Schematic representation of mesoscale atmospheric flow conditions caused by regional topography. The Niwot Ridge Ameriflux site is shown approximately 8 km West of the Continental Divide. (a) Buoyancy-driven upslope flow characteristic of summer afternoons with unstable conditions and light upper-level winds. (b) Summertime flow with low-speed Westerly winds showing mountain gravity waves that are detected at the study site. (c) Wintertime strong winds which form large mountain gravity waves that crest East of the study site. Note capping clouds that often form over the Continental Divide during moderate-to-strong Westerly flows, and lenticular clouds that form further East of the Continental Divide during large mountain wave events.

three-dimensional (CSAT-3, Campbell Scientific) or two-dimensional (Model 425A, Vaisala, Inc.) sonic anemometers. A comparison of these anemometers is given in Turnipseed et al. (2003). At the D1 meteorological station, hourly averages of wind speed and direction were recorded using a helicoid propeller anemometer mounted 10 m above the surface. Since this station was located above the tree line, there was no significant interference from vegetation. Temperature, relative humidity and barometric pressure were measured at both sites (Turnipseed et al., 2002; Losleben, 2002). Net radiation was measured at the top (25 m) level of the Ameriflux tower (model Q7.1, REBS, and model CNR-1, Kipp and Zonen).

Continuous EC fluxes of heat, momentum, $H_2O$ and $CO_2$ were measured at a height of 21.5 m ($z$

$= 1.89\,h_c$). Temperature fluctuations were measured with one of the three-dimensional sonic anemometers (CSAT-3, Campbell Scientific or ATI-K, Applied Technologies, Inc.) mounted on a horizontal boom extending 1.8 m to the South from the western edge of the tower. Water vapor fluctuations were measured with both an open path Krypton (Kr) hygrometer (KH20, Campbell Scientific) and a closed-path infrared gas analyzer (IRGA, model 6262, Li-Cor, Inc); $CO_2$ concentrations were also measured with the closed-path IRGA. A detailed physical description of these systems is given in Turnipseed et al. (2002) and Monson et al. (2002).

Signals from the sonic anemometers, Kr hygrometer and IRGA were recorded by dataloggers (CR23×, Campbell Scientific) at 10 Hz. Analog signals from the other meteorological sensors were measured at 1 Hz by dataloggers (CR23×, Campbell Scientific). All signals were sent serially to a personal computer (PC) running the Atmosphere–Surface Turbulent Exchange Research (ASTER) software package developed in the Atmospheric Technology Division (ATD) at the National Center for Atmospheric Research (NCAR) for ingesting and archiving data (Businger et al., 1990). The PC synchronized these signals in time, and then transferred them via fiber optic cable to a Sun workstation located in a trailer 600 m from the tower.

Prior to calculating turbulent fluxes, wind vectors were mathematically rotated using either the planar fit method (Wilczak et al., 2001) or by forcing the mean lateral ($\bar{v}$) and vertical ($\bar{w}$) wind velocities to zero following the procedure described by Kaimal and Finnigan (1994). We have compared these methods of rotation with no significant, observable effect on calculated heat, $H_2O$ or $CO_2$ fluxes (Turnipseed et al., 2003). Vertical fluxes were derived from the covariance between the turbulent (fluctuating) quantities of the rotated vertical wind velocity and the scalar of interest. Momentum fluxes were derived from the covariance between the $u$ and $w$ wind fluctuations ($u'w'$), friction velocities ($u^*$) were calculated as described by Stull (1988), and sensible ($H$) and latent ($\lambda_E$) heat fluxes were calculated (and corrected when necessary) as described by Webb et al. (1980) (see also Turnipseed et al. (2002) for more details). Lag times between scalars and wind velocities were determined by cross correlation and corrected during data processing.

## 4. Results and discussion

In Part 1 of this series, we discussed the local effects of topography and the forest canopy on surface fluxes and defined "local" as within the estimated source or sink footprint (Turnipseed et al., 2003). In this paper, we investigate meteorological phenomena that have their origin in events that occur at larger spatial scales (i.e., > 1 km). Mountain peaks to the North and West of the site can channel westerly winds in a way that causes extreme changes in pressure and perturbs local wind flows. Additionally, heating along mountain slopes can lead to local and regional air circulation patterns. The influence of mountain topography on regional circulation result in three broad categories of flow patterns (Barry, 1993) that can have an important impact on flux measurements: (1) formation of katabatic drainage flow in response to nighttime radiational cooling; (2) formation of anabatic flow due to daytime heating or synoptic systems; and (3) formation of mountain gravity waves as westerly winds pass over the Continental Divide (Fig. 2). All of these motions, while expressed over the scale of several $km^2$, have the potential to influence local turbulent fluxes by altering the structure of turbulence, changing footprint areas, and causing temporal variability in turbulent statistics (i.e., causing non-stationary flows). In our previous work, we investigated the first of these influences as, although drainage flows can be a large-scale phenomena, it is highly modulated by the local topography. In this work, we focus on the latter two.

### 4.1. Upslope flows and transitions between upslope and downslope regimes

We frequently observed upslope, easterly flows at the Niwot Ridge site, which are opposite to the predominant, upper-level, westerly winds. One mechanism which we observed to consistently produce upslope flow was the passage of a synoptic scale storm system, usually from a low pressure area situated on the plains southeast of the mountains. This induces counterclockwise wind flow around the low pressure area and forces air towards the Eastern slopes of the mountains. At these times the Niwot Ridge site can be in a convergence zone (denoted as the lee-side Convergence Zone, LCZ, Banta, 1984), in which the

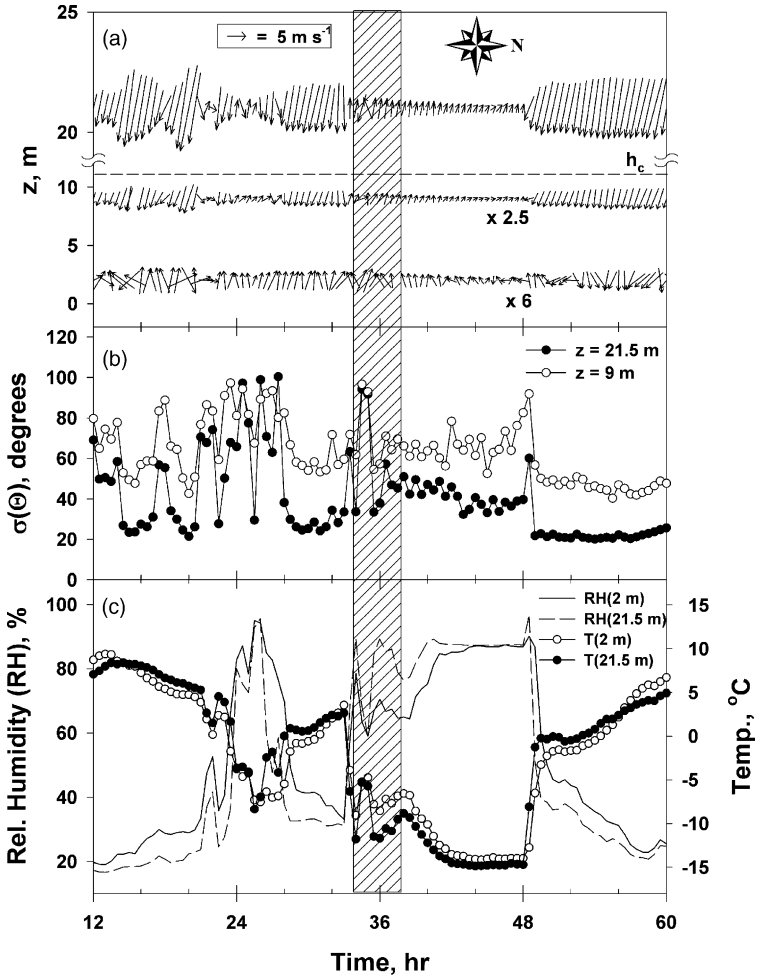


Fig. 3. Time series of (a) wind vectors, (b) standard deviation of wind direction ($\sigma_\Theta$) and (c) temperature and relative humidity starting on 12:00 noon of 1 April 2002. Hatched area denotes period when investigators were present at the site for visual observations (described in text). Measurement heights are denoted on the legend, wind vectors at $z = 9$ m are multiplied by 2.5 and those at $z = 1$ m are multiplied by 6 for visual clarity.

synoptic airflow moving upslope from the East converges with the higher-level westerly winds. Within this zone, the wind flows transition back and forth causing non-stationarity within the half-hour time block required for flux averaging. An example of such an extended LCZ event occurred during a 2 day period in April, 2002 (Fig. 3) when an upslope flow from a storm system converged with westerly flow near the elevation of the measurement tower. While the lowest sampling height indicated upslope (easterly) flow, winds above the canopy were downslope. However, there were intermittent periods when the upslope flow moved to higher sampling levels. These transitions were marked with high variability in wind direction (Fig. 3b) and large shifts in humidity and temperature (Fig. 3c). Visual observations during a portion of the period (marked on figure) showed cold, moist flows (fog) moving upslope within the canopy while skies above the canopy remained clear and exhibited downslope flow. These periods of sustained, radical wind direction differences appear to be rare, as less than 3% of the time periods between April, 2002 and February, 2003 had consistent counter-undercanopy flow for periods longer than 2 h.

A second mechanism that often induced upslope flow was heating along the slope (see Banta and Cotton, 1981; Banta, 1984). These are typically known as mountain/valley breezes. During daytime periods in which synoptic forcing was absent, anabatic (or upslope) flow was still commonly observed (~33% of all half-hour daytime periods during the summer of 2001). These periods were characterized low wind speeds and strong surface heating (as indicated by high atmospheric instability). In winter when surface heating was low and the predominant Westerlies were stronger, these buoyancy-driven flows were much less common. One event typical of midday anabatic flow was observed on 12 August 2001 (Fig. 4a). Just before noon, the wind direction recorded at 1 m shifted from westerly to easterly. This occurred soon after the temperature within the canopy became warmer than that above. The appearance of the upslope wind was first noted at the lowest sampling height, and affected the highest sampling height approximately 1 h later; 2 h later, the upslope wind reached the D1 meteorological tower (8 km upslope). We observed tight coupling of the anabatic flow with net radiation ($R_{net}$) and temperature (Fig. 4b and d). As clouds moved over the site, and $R_{net}$ and, subsequently, temperature decreased, the anabatic wind lost strength, and downslope katabatic (drainage) flows would initiate at $z = 1$ m. Clearly, thermally-induced upslope flows can

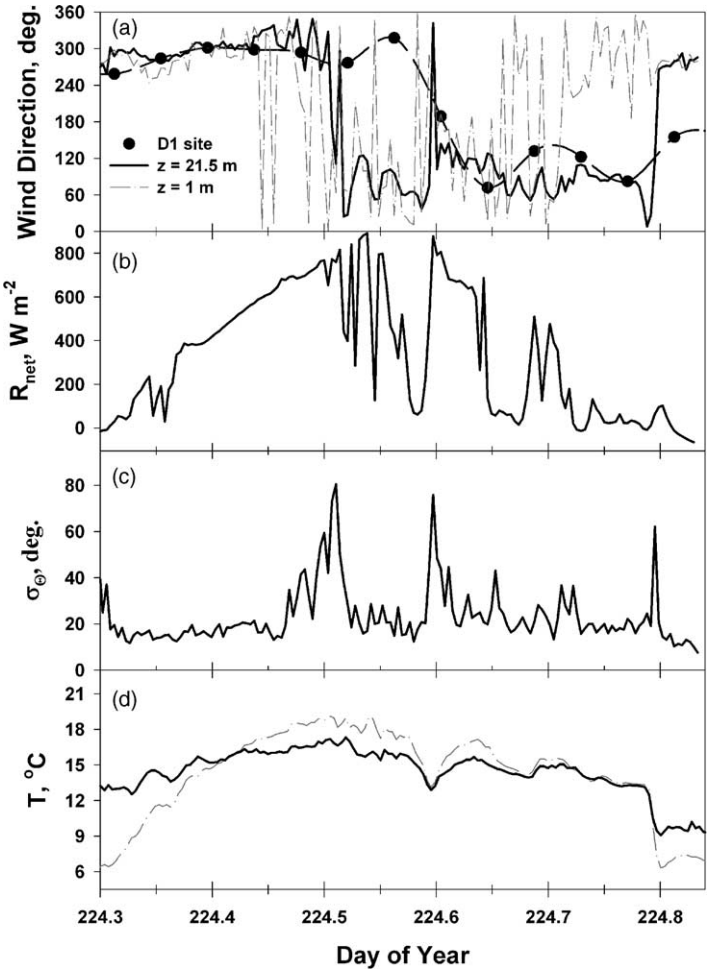


Fig. 4. Daytime time series of (a) wind direction (b), net radiation, (c) standard deviation of the wind direction and (d) temperature for a typical upslope day (12 August 2001). Tower data represent 5 min averages. Data from D1 are 1 h averages.

exhibit a rather fast response to local conditions, as has been observed previously (Kossman and Fiedler, 2000). Eventually, anabatic flow ceased at the tower site as the stable nighttime boundary layer appeared.

The passage of the buoyancy-driven upslope flow led to marked peaks in the variability of the wind direction ($\sigma_\Theta$, Fig. 4c), which were often accompanied by peaks in $u^*$ (data not shown), presumably caused by wind sheer between atmospheric layers. In principle, a rapid change in mean wind direction can cause a violation of stationarity as turbulent statistics (variances of wind components, etc.) can change with time. This results in inadequate sampling of all of the turbulent scales contributing to the flux during a given averaging period (typically 30 min in this study). This non-stationarity in the wind flow will have its largest impact felt on the momentum flux and can affect the scalar fields if the time rate of change of these scalars changes or if the site is not very homogeneous. Since buoyancy-driven upslopes are frequent in summer, it is important to determine how often these wind transitions occur since these flows can cause non-stationarity and subsequent errors in local turbulent flux determinations.

Initially, we used $\sigma_\Theta$ as an indicator of non-stationary wind flow (see Fig. 4c). This approach was non-specific with regard to cause of the upslope/downslope transition (i.e., whether it was due to synoptic storm activity or surface heating). Vickers and Mahrt (1997) used a similar test based on the ratio of the vector-averaged wind speed to the scalar average wind speed ($\vec{U}/U$); periods with $\vec{U}/U \leq 0.9$ were considered questionable and marked for further scrutiny. We found that $\vec{U}/U$ was highly correlated with $\sigma_\Theta$ (i.e., time periods with $\vec{U}/U \leq 0.85$ also exhibited $\sigma_\Theta \geq 40^\circ$). For the summer of 2001 (June–August), we observed that 26% of the total daytime half-hour measurement periods had $\sigma_\Theta > 40^\circ$ (see Table 1). Many of these were associated with downslope/upslope transitions. Table 1 shows the results of applying the stationarity tests described by Foken and Wichura (1996) using either sensible heat or momentum flux as surrogates. As expected, momentum fluxes were more susceptible to the wind flow variability, showing a higher percentage of violations (36%). Scalar fluxes (sensible heat) were also affected by variable wind directions, but to a lesser degree, suggesting a more uniform scalar field (both spatially and temporally). This was also borne out in the observation that energy budget closure showed no discernible dependence with $\sigma_\Theta$. Therefore, the impact of these periods of highly variable wind direction to the long-term scalar flux record appears to be insignificant.

Table 1
Stationarity violations caused by upslope/downslope transitions

| | $\sigma_\Theta > 40^\circ$ | $\sigma_\Theta < 40^\circ$ |
|---|---|---|
| Number of periods (% of total)[a] | 519 (26%) | 1477 (74%) |
| % of stationarity violations[b] | | |
| $u'w'$ | 36% | 4% |
| $w'T'$ | 25% | 13% |

[a] Data was taken from June–August, 2001, daytime periods only ($R_{net} > 20\,W\,m^{-2}$).

[b] Stationarity was assessed following the recommendations of Foken and Wichura (1996) where the average flux obtained from 5 min subrecords (within a 30 record) was compared to the flux obtained from the total 30 min record. Differences greater that ± 30% constituted a violation of stationarity.

A more difficult question lies in the impact these upslope flows have in creating low frequency or advective fluxes at the Niwot Ridge site. Several past studies have noted that large-scale circulations can be tied to the surface heterogeneity and topography (Doran et al., 1992; Mahrt et al., 1994; Sun et al., 1997). These can create large quasi-stationary eddies that are stable on hourly time scales (Mahrt, 1998), creating steady advection during those time periods. A mountain/valley flow is a prime example of this type of surface/atmosphere interaction. In our previous work, (Turnipseed et al., 2002), we observed lower average energy budget closure during periods with upslope flow as opposed to those with downslope flow. We concluded that advection was a likely source of this discrepancy and likely played a role in the overall imbalance between available energy and turbulent fluxes. We revisit this topic here in light of the recent work by Finnigan et al. (2003), whose method includes contributions from horizontal advection, averaged over longer time periods. Individual half-hour fluxes of sensible and latent heat for the summer of 2002 (June–August) were combined into longer averaging periods (2–12 h). Coordinates within each half-hour subrecord were rotated using the planar fit method (Wilczak et al., 2001), such that the vertical velocity vector was aligned perpendicular to that of the long-term mean flow streamlines. Fluxes

for the longer averaging periods were derived by the ensemble average of the turbulent fluxes, ($\overline{w'c'}$), and (2) via the equation

$$\langle \overline{wc} \rangle = \langle \bar{w}'\bar{c}' + \overline{w'c'} \rangle \quad (1)$$

where $\bar{w}' = \bar{w}_i - \bar{w}_{LT}$, and $\bar{w}_{LT}$ is the "long-term" mean obtained by averaging over the 2–12 h period and $\bar{w}_i$ is the mean for the individual half-hour subrecord. Similarly, $\bar{c}' = \bar{c}_i - \bar{c}_{LT}, \bar{c}_{LT} = \frac{1}{N}\sum_{i=1}^{N}\bar{c}_i$ where $N$ is the total number of half-hour subrecords. From Finnigan et al. (2003), the term $\bar{w}'\bar{c}'$ carries both the low frequency component of the flux and any transient horizontal flux divergence below the measurement height (caused by flow divergence or convergence at shorter time periods). When averaged over the longer time period, the transient horizontal advection cancels out, leaving just the low frequency contributions (Finnigan et al., 2003). Fig. 5 shows a plot of average latent heat fluxes derived via Eq. (1) versus the ensemble-averaged half-hour turbulent flux. No significant enhancement of either the sensible or latent heat fluxes were observed (< 2%) until averaging periods of 12 h (or more) were employed. This was independent of mean wind direction over the averaging

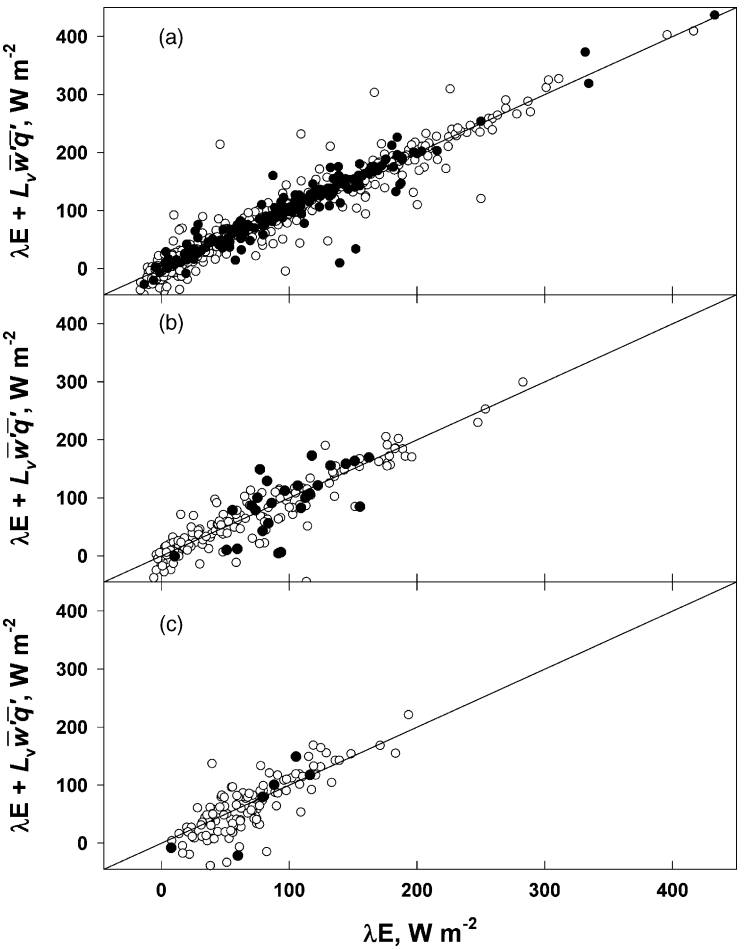


Fig. 5. Plots of latent heat flux corrected for low frequency fluxes according to Eq. (1) vs. uncorrected latent heat fluxes for (a) 2 h, (b) 8 h and (c) 12 h averaging times. Data is for the summer (June–August) of 2002. Solid circles represent time periods in which wind directions were upslope (60–200°). Lines drawn are the 1:1 line. Least squares regression slopes for the three plots were $m = 1.00$, 1.03 and 1.14 for plots (a), (b) and (c), respectively.

period. A 12 h averaging period led to a 14% increase in latent heat flux, but essentially no increase in sensible heat flux. However, there are few buoyancy-driven upslope winds that are maintained over a 12 h period so that a comparison between upslope and downslope flow conditions becomes inconsequential. In fact, it is likely that the enhancement we found at the 12 h averaging times was, at least in part, due to the low frequency flux contributions caused by diurnal shifts between upslope and downslope wind regimes. For a 2 h averaging period, this lack of low frequency contributions was corroborated by examining co-spectra for heat, $H_2O$ and $CO_2$ fluxes, as a function of wind direction. We found that, although there were significant contributions to the flux at frequencies less than 0.002 Hz, there was no difference in this spectral region between upslope and downslope periods (data not shown). Therefore, it appears that low frequency contributions to the fluxes are not preferentially larger for upslope relative to downslope wind flows.

### 4.2. Mountain gravity waves

One of the primary mechanisms for the movement of mass and energy in the stable nighttime boundary layer is the propagation of waves. Waves of various sizes have been noted within stable boundary layers (Finnigan et al., 1984; Paw et al., 1990; Fitzjarrald and Moore, 1990; Sun et al., 2002), however, they are often obscured by shear-generated turbulence (especially over tall canopies) near the surface. During calm, stable conditions, recent work has shown the regular occurrence of gravity waves over canopies (Lee et al., 1997; Lee and Barr, 1998). At the Niwot Ridge site, we have observed periodic canopy wave formation during stable periods similar to that described in the studies by Lee and coworkers; however, we have also seen evidence of lower frequency gravity waves, likely initiated by the large-scale mountainous topography surrounding the site (Barry, 1993; Stull, 1988).

Fig. 6 shows time series data for vertical velocity, $CO_2$ and temperature for a 2 h period during highly stable nighttime conditions ($z/L > 1$, where $L$ is the Obukhov length). Turbulent "bursts" occurred approximately every 20 min and were indicated by an increase in the standard deviation of the vertical velocity ($\sigma_w$). Concurrent with increased $\sigma_w$ were larger fluctuations in temperature and $CO_2$ (similar fluctuations were also noted in mean wind speed and water vapor). Clearly, a low frequency, periodic fluctuation was observed, which we interpret as a mountain gravity wave that likely propagated downhill past the tower site. Embedded within the low frequency wave, subperiods can be identified which contain higher frequency waves (shown in the insets of Fig. 6) each with periods of ~15–25 s. These waves appear similar to those described previously for a mixed coniferous/broadleaf forest (Lee et al., 1997) and are likely generated in a shear layer near canopy height.

Evidence of both wave structures was corroborated by spectral analysis. Power spectra of $w$ and temperature for the 2 hr period indicated prominent peaks at 0.0008 Hz ($\tau = 1250$ s or 20.8 min) and 0.04 Hz ($\tau = 25$ s) (Fig. 7). Using the measured average wind speed of 3.1 m s$^{-1}$, we estimated a wavelength ($\lambda_l$) of 3.9 km for the low frequency wave. This length should be considered a lower limit as our observation height is likely below the critical height where phase speed (the speed at which the wave is propagated) equals wind speed. This wavelength can be used to estimate the Froude number for this wave episode assuming that $\lambda_l = U/N_{BV}$ (Stull, 1988; Barry, 1993; Kaimal and Finnigan, 1994)):

$$F_L = \frac{U}{N_{BV} L_h} = \frac{\lambda_l}{L_h} \quad (2)$$

where $N_{BV}$ is the Brunt-Väisälä frequency (Kaimal and Finnigan, 1994) and $L_h$ is the half-width at half-height of the hill/mountain which perturbs the airflow. Assuming $L_h \sim 15$ km (the estimated half-width at half-height from the Continental Divide to Boulder, CO, see Fig. 1) yielded $F_L \sim 0.26$; implying fairly strong stability and low to moderate wind speeds through the stable boundary layer (Stull, 1988), which is consistent with conditions observed at the surface.

The observation of waves (both low and mid-frequencies) poses a difficult problem for turbulent flux measurements. Hu et al. (2002) have shown through numerical simulation that there is no constant flux layer during wave events. Sun et al. (2004) have also shown how wave action can lead to temporary instabilities, intermittent turbulent mixing and fluxes that are counter to the time-averaged gradient. As seen in Fig. 7, large contributions to the power spectra were observed at the wave frequencies (both

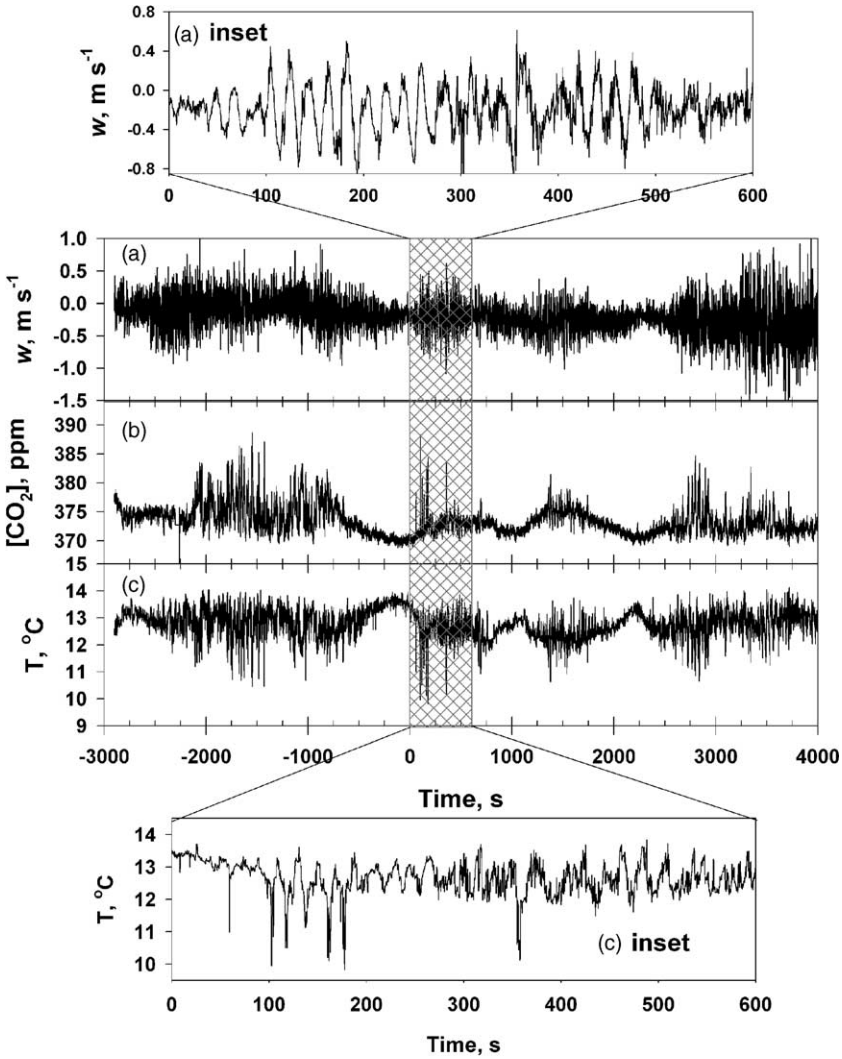


Fig. 6. Two-hour time series of (a) vertical wind velocity, $w$, (b) [$CO_2$], and (c) temperature, $T$ on the night of 25 August 2001 beginning at 0:00 MDT. Evidence of longer period waves occurring between 0 and 3000 s suggest the presence of mountain waves. Time series for $w$ and $T$ within the shaded region is expanded in the insets showing evidence of higher-frequency canopy waves.

low and mid-frequencies) for both $w$ and scalars. Integration of the co-spectra indicated that between 25 and 50% of the total scalar ($T$, $q$) covariance was accounted for within the low frequency wave (Fig. 7b); indicating prominent influences of the waves on local fluxes during these times. At the very least, the observed co-spectra imply a re-assessment of the averaging period length: either longer averaging times in order to adequately sample fluxes during wave events, or shorter averaging periods to take advantage of the spectral gap observed between the low and mid-frequencies waves (see Vickers and Mahrt, 2003).

Using potential temperature and wind speeds measured at 21.5 and 8.0 m, we calculated the gradient Richardson's number ($R_i$) of 0.32 for the time period shown in Fig. 6. Although $R_i$ was measured within the roughness sublayer, not the surface layer, it still appears to be a relatively robust measure of stability near the canopy. This value of $R_i$ is above the critical value ($R_{ic}$) of 0.25 necessary to support wave for-

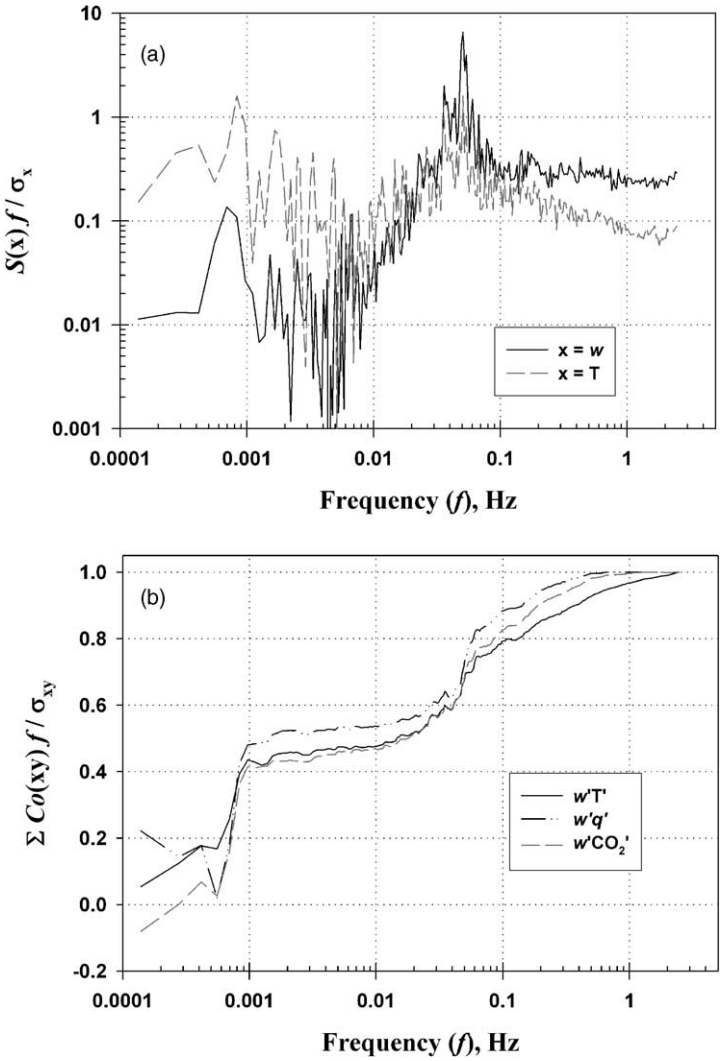


Fig. 7. (a) Power spectra of $w$, and temperature for the time period shown in Fig. 6. The spectrum is multiplied by frequency and normalized by the variance. (b) Cumulative co-spectra for temperature ($w'T'$), $H_2O$ vapor ($w'q'$) and $CO_2$ ($w'CO_2'$) for the 2 h time period shown in Fig. 6.

mation (Finnigan et al., 1984; Stull, 1988). Using $R_i$, an analysis of 10 months of data (March–December, 2002) indicated that 33% of the nocturnal periods had $R_i > 0.25$. There was somewhat of a seasonal cycle with a higher percentage of points during the summer months when lower wind speeds and higher stability were more likely. Use of the Richardson's number was only a crude filter for wave occurrence as visual screening of many of these time periods indicated no observable low frequency wave formation. A spectral screening method such as that described by Lee and Barr (1998) was also attempted. This proved successful for mid-frequency canopy waves; however, in the low frequency ($f \sim 0.0005$–$0.001$ Hz) region, other sources of non-stationarity were often seen to produce spectral strength, and further study is needed in order to ascertain the percentage of nocturnal periods affected by these low frequency waves.

As wind speeds increase, observation of large waves at the surface within the wind or scalar time

series becomes obscured by mechanically-generated turbulence. However, numerous studies have observed evidence of larger waves in mountainous topography during periods of moderate to strong prevailing winds (Lilly and Zipser, 1972; Brinkman, 1974; Barry, 1993; Ralph et al., 1997). These conditions are fairly typical in wintertime at the Niwot Ridge tower site. Visible evidence of lee-side waves includes the presence of "capping clouds" over the peaks of the Continental Divide and the formation of downwind lenticular clouds that form at the crests of the waves, and roll clouds beneath them (see Fig. 2c). Intuitively, the wavelength and amplitude of lee-side waves will vary depending upon wind speed, lapse rate (or stability) and boundary layer height. When the Froude number is near unity ($F_L \sim 1$), the wavelength of the perturbed air flow will be nearly equal to $L_h$, thus causing a resonance enhancement of the wave amplitude. These conditions can generate large trapped lee-side waves that can result in downslope windstorms characterized by high wind speeds, strong turbulence, and the possible formation of rotor winds beneath the crests of the waves (Lilly and Zipser, 1972; Brinkman, 1974; Barry, 1993). There is a plethora of possible situations on either side of $F \sim 1$, ranging from a single standing wave ($F_L < 1$) to rotor streaming ($F_L > 1$) (Barry, 1993).

At the Niwot Ridge site we typically observed high average wind speeds ($U \sim 8$–$20\,m\,s^{-1}$) and large friction velocities ($u^* > 1.3\,m\,s^{-1}$) when capping clouds or other visual evidence of large-scale wave formation was present. Recent modeling of mountain-induced waves shows that pressure gradients on the lee sides of mountain ridges can create a region of shallow, high velocity, "shooting flow" on the downslope side of a ridge just prior to steamline separation (Doyle and Durran, 2002). Past studies of mountain waves near the Niwot Ridge site (Brinkman, 1974; Ralph et al., 1997) have reported wavelengths of $15.8 \pm 4.5$ km for 24 different events in which trapped lee-side waves were present (approximately equal to $L_h$ as expected from $F_L \sim 1$). This places the crests of the waves approximately 8 km to the East of our site. Thus, for most of the large mountain wave events, the Niwot Ridge site is in the "shooting flow" regime of the wave structure.

The "shooting flow" regime of the large mountain waves is not likely to cause significant errors in the estimation of local eddy fluxes. We have observed these high wind periods to be highly stationary (in both speed and direction) for several consecutive hours. These periods also tend to exhibit valid turbulence statistics ($\sigma_w/u* \sim 1.25$) as expected in the neutrally-stratified surface layer, consistent with similarity theory (Kaimal and Finnigan, 1994). We have also previously reported nearly complete closure of the surface energy budget during these periods (Turnipseed et al., 2002). Therefore, it appears that as long as the flux tower (and surrounding fetch) is within the shooting flow regime, and upstream of wave crests, flux measurements remain representative of the surrounding surface.

However, there are time periods when we observed large variability in wind direction and speed suggesting the possible presence of a quasi-stationary recirculation (see Fig. 8). For near-surface flux measurements, this recirculation, or rotor, could cause several complications. The presence of such an organized structure in the surface layer (with one area experiencing a long period updraft and another, a long period downdraft) may result in: (1) a surface layer that is not horizontally homogeneous, and (2) loss of a constant flux layer. It would also be conceivable that the air sensed at the tower site may have insufficient contact with the surface before measurement (i.e., it is transported directly down from aloft in the downward-moving limb of the rotor). This would result in insufficient exchange of mass and energy with the surface and would be expected to lead to a decrease in the measured turbulent exchange. Full assessment of the mechanisms of flux loss due to recirculation patterns at the Niwot Ridge site is beyond the scope of this paper; we would need measurements of airflows across much larger vertical and horizontal spatial scales. However, we were able to assess the frequency of rotors, and understand some of the implications on local turbulent fluxes measured at the tower site during rotor events.

We have looked at simultaneous time series data for wind speed and direction from the Ameriflux tower and the D1 meteorological site as a means of identifying rotor occurrence. For this analysis we used data from December 2000–March 2001, as lee wave formation is more prevalent during the winter months. Also, since a recirculation flow could appear as an upslope wind, the presence of rotors can be more frequently confused with a buoyancy-driven upslope flow during the summer as compared to the winter. However, it

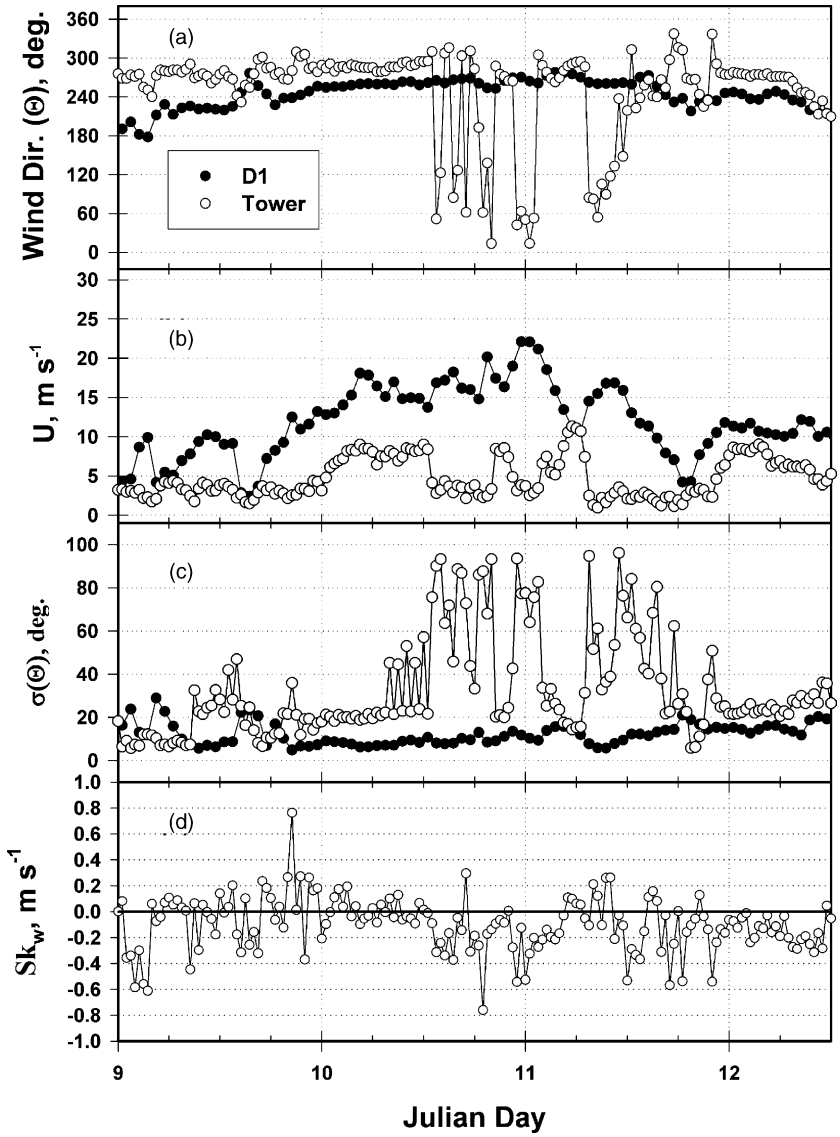


Fig. 8. Time series of half-hour average (a) wind direction ($\Theta$), (b) speed ($U$), (c) standard deviation of wind direction, ($\sigma_\Theta$), and (d) the skewness of $w$ ($\mathrm{Sk}_w$) for 9–13 January 2001. Measurements are taken from the Niwot Ridge Ameriflux tower and the D1 meteorological site. Rotor occurrence is thought to occur during the periods when large differences in wind direction existed between the tower and D1.

should be noted that rotor formation requires strong winds near the crest of the ridge ($> 8\,\mathrm{m\,s^{-1}}$, Nicholls, 1973), whereas buoyancy-driven upslopes are only observed when the predominant winds are weak. Fig. 8 shows the time series data for wind speed and direction during one possible rotor event. Wind speed at the D1 site remained high ($> 10\,\mathrm{m\,s^{-1}}$) and the direction remained from the West throughout the event. At the Ameriflux tower, 8 km downslope from the D1 site, wind direction began to fluctuate between upslope and downslope for a continuous stretch of nearly 24 h. Comparisons of wind speeds at D1 and the tower shown in Fig. 8 indicated that they were initially positively correlated. At the onset of the possible rotor, wind speeds at the two sites became anti-correlated. Within the stationary rotor, near the surface, wind

speed would be expected to be low (Ralph et al., 1997), and the standard deviation of wind direction would be expected to be high, both of which were observed at the Ameriflux tower (Fig. 7c). Although, not conclusive (as we do not have complete vertical profile data through the boundary layer), these observations do suggest the likelihood of a rotor wind positioned over the Ameriflux tower site.

By looking at differences in wind speed and absolute wind direction between the Ameriflux tower and the D1 site, it is possible to estimate the number of half-hour measurement periods at the Ameriflux site that could be influenced by rotor winds (Fig. 9). After data were initially screened for wind speed at D1 ($U > 8\,\mathrm{m\,s^{-1}}$), differences in wind direction between D1 and the tower site were investigated. Only 14% of the 30 min averaged time periods that we examined for December 2000–March 2001 showed large differences in direction (>50°) between the two measurement locations and strong winds at the D1 site. The criteria of high wind speed at the crest effectively eliminates most periods exhibiting buoyancy-driven upslopes, which are characterized by low wind speeds. A similar analysis of summer data (June–August, 2001) indicated that possible rotor occurrence dropped to less than 3% of the half-hour time periods during that summer season. We also noted that 68% of the time periods (summer and winter data) with possible rotor events occurred at night when convective activity was minimal. This also is in agreement with past studies on trapped lee waves, which suggest that as stability increases, the wavelength decreases (Barry, 1993); thus leading to wave crests closer to the ridge crest and the tower site.

Analysis of the vertical wind velocity indicated large variability in $\bar{w}$ during the time periods in which rotor activity was likely; however, there were no discernible trends in $\bar{w}$. Of the rotor periods analyzed, it did appear that the skewness of the $w$-distribution tended to be more negative, suggesting intermittent pulses of strong downward-moving air (Fig. 7d). This would tend to suggest that we were possibly on the downward-moving limb of the rotor during these periods.

Since rotor formation can potentially influence several basic tenets of surface layer flux measurements, it is informative to determine if measurements at a single tower location can be used to flag potentially invalid data. As mentioned above, large variability in wind directions were highly correlated with rotor occurrence at the site (see Fig. 7c). The standard deviation of wind direction proved to be the most reliable parameter in data screening. Of the time periods shown in Fig. 8

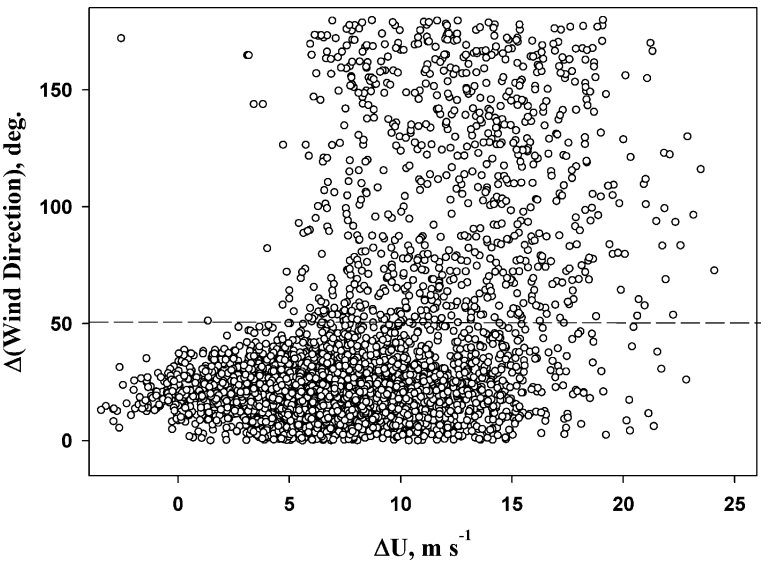


Fig. 9. Plot of the absolute difference in wind direction (Δ: wind direction; $|\Theta_{D1}-\Theta_{tower}|$) vs. the difference in wind speed ($\Delta U$: $U_{D1}-U_{tower}$) between the Niwot Ridge Ameriflux tower site and the D1 meteorological site during December 2000–March 2001.

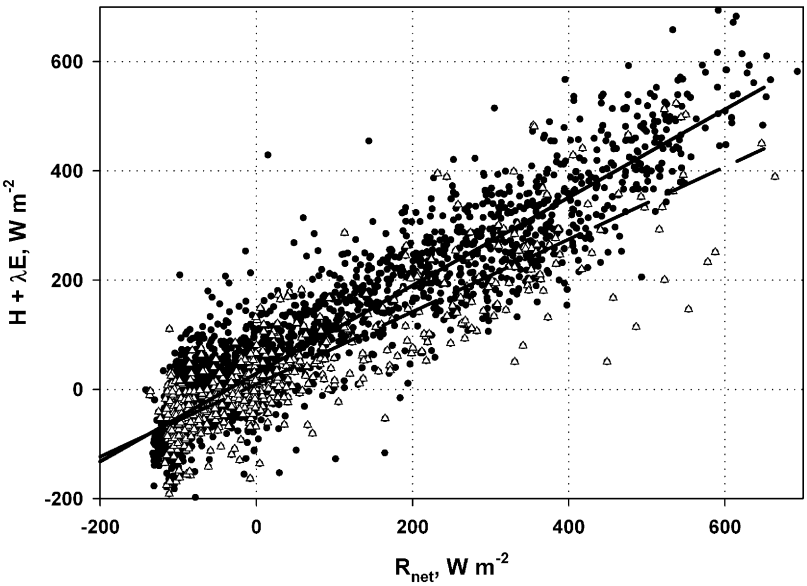


Fig. 10. Plot of the energy budget $\{(H + \lambda E)$ vs. $R_{net}\}$ for the time period shown in Fig. 9. Solid circles denote periods when wind direction differences between the flux tower and the D1 site were less than 50°, open triangles denote differences larger than 50°. Solid line is the regression line for the solid circle points, dashed line is the regression line for open triangle points.

which have a difference in wind direction of at least 50° between the Ameriflux and D1 sites, nearly 80% have $\sigma_\Theta > 40°$. Thus, analysis of the standard deviation of wind direction can be used as a reliable indicator of suspected rotor activity. It was often noted that peaks in $\sigma_w/u*$ were observed when rotors were either initiated or subsided. However, during periods when the rotor was established, turbulence statistics were often within reasonable bounds as set by Foken and Wichura (1996). Finally, it was observed that during periods with suspected rotor activity, energy budget calculations indicated substantially lower closure (20% less, Fig. 10) and a greater degree of scatter relative to surrounding time periods. Mean $CO_2$ fluxes were also lower during these suspected periods by ∼30%. The use of a "mean" $CO_2$ flux is a reasonable proxy, because the soil temperature remains nearly-constant due to snow coverage, which results in nearly-constant, positive fluxes during the winter months. Substitution of the mean $F(CO_2)$ during un-affected periods into rotor-affected time periods resulted in a 6% increase in cumulative $CO_2$ released from the site. The exact mechanism for the loss of flux is uncertain as there could be multiple possibilities (such as incomplete equilibration of the airflow with the surface, increased horizontal advection, changing fetch, etc.), and this remains a topic of further study. However, the negative impact of rotor activity on measured turbulent fluxes was observed in both energy and $CO_2$ fluxes, but the low occurrence rate (∼3–14%) results in a small impact on long-term flux measurements at this site.

## 5. Conclusions

Regional air flow patterns are strongly affected by the surrounding mountain topography and can play an important role in local flux determinations. Large-scale motions can lead to local nonstationarities in the turbulent field, formation of horizontal advection and inefficient coupling between the mean flow and the underlying surface. These can manifest themselves as a loss of turbulent flux at a particular point (such as the tower site). We have attempted to identify flow patterns that are common in mountainous regions that could lead to possible local turbulent flux loss and determine: (1) the frequency of their occurrence and

(2) the impact on the local eddy flux measurements and the long-term flux record.

One of the most frequent causes of non-stationarity in the turbulence field was the formation of alternating upslope and downslope flows. However, only 26% of summer, daytime time periods indicated these altering flows and an even smaller fraction (10%) indicated nonstationarities in the eddy flux measurements (when using the criteria described by Foken and Wichura, 1996). There was also no indication of scalar flux loss during periods with high degrees of wind direction variability as denoted by similar energy budget closure. We have also attempted to deduce the degree of horizontal advection which may be present with these flows using the analysis described by Finnigan et al. (2003), but have also found these effects to be minimal (14% for $\lambda_E$, essentially no flux enhancement for sensible heat) as well. Therefore, it appears that long-term flux measurements are only slightly affected by the occurrence of summertime, buoyancy-driven upslope flow.

We found evidence for the formation of lee gravity waves with a period of ∼20 min that affected the turbulence field above the canopy; higher-frequency canopy waves were also observed, often embedded within the larger waves. Low frequency waves suggest that a re-evaluation of our averaging periods may be needed so that flux contributions from low frequency are not excluded, or to exclude measurements during these periods. Larger lee waves were observed during the winter in the presence of stronger wind velocities. The Niwot Ridge Ameriflux tower site likely resides within the "shooting flow" regime of these larger waves during most events. Analysis of time series data revealed high friction velocities, neutral atmospheric stability and no evidence of compromise in the local turbulent flux measurements within the "shooting flow" regime. Using data from a second site upwind, we observed evidence of rotor winds at the tower site, but they were conservatively estimated to occur in only 14% of the wintertime half-hour flux periods. Without data from more than one location or from planetary boundary layer profiles, it is impossible to unambiguously ascertain the presence of rotor winds; however, the standard deviation in wind direction tended to flag the majority (∼80%) of the time periods when there was the possibility of rotors. Losses in local turbulent fluxes were apparent during periods with suspected rotors in both energy fluxes (lower energy budget closure by ∼20%) and $CO_2$ fluxes (30% decrease from the average for the 4 month period investigated).

In each of the cases investigated (upslope transitions or rotor winds), it appears that inspection of the standard deviation of the wind direction at the tower site can be used as a reliable indicator to flag events and filter those that violate stationarity from the data record.

## Acknowledgements

The authors would like to thank the other members of the Monson research group for their assistance and contributions. Dr. Dave Bowling provided invaluable help during early stages of the project. The authors would also like to thank members of the Atmospheric Technology Division of the National Center for Atmospheric Research for assistance and guidance in establishing this research site and the data acquisition system. Special thanks are offered to Dr. Tony Delany, Gordon McLean, and Dr. Steve Oncley for their time and efforts. The authors would also like to thank Dr. Bill Bowman at the University of Colorado Mountain Research Station and Mark Loesleben and Todd Ackerman of the Niwot Ridge Long-Term Ecological Research (LTER) site for access and help with the D1 data. Finally, we would like to thank the US Forest Service for permitting the establishment of the research site in the Roosevelt National Forest. This research was funded by the South Central Section of the National Institute for Global Environmental Change (NIGEC) through the US Department of Energy and the Terrestrial Carbon Processes (TCP) Program of the Biological and Environmental Research (BER) Division of the US Department of Energy.

## References

Aubinet, M., Grelle, A., Ibrom, A., Rannik, U., Moncrieff, J., Foken, Th., Kowalski, P., Martin, P., Berbigier, P., Bernhofer, Ch., Clement, R., Elbers, J., Granier, A., Grunwald, T., Morgenster, K., Pilegaard, K., Rebmann, C., Snijders, W., Valentini, R., Vesala, T., 2000. Estimates of the annual net carbon and water exchanges of European forests: the EUROFLUX methodology. Adv. Ecol. Res. 30, 113–174.

Baldocchi, D.D., Falge, E., Gu, L., Olson, R., Hollinger, D., Running, S., Anthoni, P., Bernhofer, Ch., Davis, K., Evans,

R., Fuentes, J., Goldstein, A., Katul, G., Law, B., Lee, X., Malhi, Y., Meyers, T., Munger, W., Oechel, W., Paw, U.K.T., Pilegaard, K., Schmid, H.P., Valentini, R., Verma, S., Vesala, T., Wilson, K., Wofsy, S., 2001. FLUXNET: a new tool to study the temporal and spatial variability of ecosystem-scale carbon dioxide, water vapor and energy flux densities. Bull. Am. Meteorol. Soc. 82, 2415–2434.

Banta, R.M., 1984. Daytime boundary-layer evolution over mountainous terrain. Part I: observations of the dry circulations. Monthly Weather Rev. 112, 340–356.

Banta, R., Cotton, W.R., 1981. An analysis of the structure of local wind systems in a broad mountain basin. J. Appl. Meteorol. 20, 1255–1266.

Barry, R.G., 1973. A climatological transect on the East slope of the front range, Colorado. Arct. Alp. Res. 5, 89–110.

Barry, R.G., 1993. Mountain Weather and Climate, Metheun & Co., New York.

Brazel, A., Brazel, P., 1983. Summer diurnal wind patterns at Niwot Ridge, CO. Phys. Geog. 4, 53–61.

Brinkman, W.A.R., 1974. Strong downslope winds at Boulder, Colorado. Monthly Weather Rev. 102, 592–602.

Businger, J.A., Dabberdt, W.F., Delany, A.C., Horst, T.W., Martin, C.L., Oncley, S.P., Semmer, S.R., 1990. The NCAR atmosphere–surface turbulent exchange research (ASTER) facility. Bull. Am. Meteorol. Soc. 71, 1006–1011.

Desjardins, R.L., MacPherson, J.I., Mahrt, L., Schuepp, P., Pattey, E., Neumann, H., Baldocchi, D., Wofsy, S., Fitzjarrald, D., McCaughey, H., Joiner, D.W., 1997. Scaling up flux measurements for the Boreal forest using aircraft-tower combinations. J. Geophys. Res. 102, 29125–29133.

Doran, J.C., Barnes, F.J., Coulter, R.L., Crawford, T.L., Baldocchi, D.D., Balick, L., Cook, D.R., Cooper, D., Dobosy, R.J., Dugas, W.A., Fritschen, L., Hart, R.L., Hipps, L., Hubbe, M., Gao, W., Hicks, R., Kirkham, R.R., Kunkel, K.E., Martin, T.J., Meyers, T.P., Porch, W., Shannon, J.D., Shaw, W.J., Swiatek, E., Whiteman, C.D., 1992. The boardman regional flux experiment. Bull. Am. Meteorol. Soc. 73, 1785–1795.

Doyle, J.D., Durran, D.R., 2002. The dynamics of mountain-wave-induced rotors. J. Atmos. Sci. 59, 186–201.

Finnigan, J.J., Einaudi, F., Fua, D., 1984. The interaction between an internal gravity wave and turbulence in the stably-stratified nocturnal boundary layer. J. Atmos. Sci. 41, 2409–2436.

Finnigan, J.J., Clement, R., Malhi, Y., Leuning, R., Cleugh, H.A., 2003. A re-evaluation of long term flux measurements techniques, Part I: averaging and coordinate rotation. Bound-Layer Meteorol. 107, 1–48.

Fitzjarrald, D.R., Moore, K.E., 1990. Mechanisms of nocturnal exchange between the rain forest and atmosphere. J. Geophys. Res. 95, 16839–16850.

Foken, Th., Wichura, B., 1996. Tools for the quality assessment of surface-based flux measurements. Agric. For. Meteor. 78, 83–105.

Hu, X., Lee, X., Steven, D.E., Smith, R.B., 2002. A numerical study of nocturnal wavelike motion in forests. Bound-Layer Meteorol. 102, 199–223.

Ives, J.D., Messerli, B., Spiess, E., 1997. In: Messerli, B., Ives, J.D. (Eds.). Mountains of the World-A Global Priority in Mountains of the World-A Global Priority, Parthenon Publishing Group, New York.

Kaimal, J.C., Finnigan, J.J., 1994. Atmospheric Boundary Layer Flows: Their Structure and Measurement, Oxford University Press, Oxford.

Kossman, M., Fiedler, F., 2000. Diurnal momentum budget analysis of thermally induced slope winds. Meteorol. Atmos. Phys. 75, 195–215.

Lee, X., Neumann, H.H., Den Hartog, G., Fuentes, J.D., Black, T.A., Mickle, R.E., Yang, P.C., Blanken, P.D., 1997. Observation of gravity waves in a boreal forest. Bound-Layer Meteorol. 84, 383–398.

Lee, X., Barr, A.G., 1998. Climatology of gravity waves in a forest. Q.J.R. Meteorol. Soc. 124, 1403–1419.

Lilly, D.K., Zipser, E.J., 1972. The front range windstorm of January 11, 1972: a meteorological narrative. Weatherwise 25, 56–63.

Losleben, M., 2002, http://culter.colorado.edu:1030/Niwot/NiwotRidgeData/D1.html.

Mahrt, L., 1998. Flux sampling errors for aircraft and towers. J. Ocean. Atmos. Tech. 15, 416–429.

Mahrt, L., Sun, J., Vickers, D., MacPherson, J.I., Pederson, J.R., Desjardins, R.L., 1994. Observations of fluxes and inland breezes over a heterogeneous surface. J. Atmos. Sci. 51, 2165–2178.

Massman, W.J., Lee, X., 2002. Eddy covariance flux corrections and uncertainties in long-term studies of carbon and energy exchanges. Agric. For. Meteorol. 113, 121–144.

Monson, R.K., Turnipseed, A.A., Sparks, J.P., Harley, P.C., Scott-Denton, L.E., Sparks, K., Huxman, T.E., 2002. Carbon sequestration in a high-elevation subalpine forest. Global Change Biol. 8, 1–20.

Nicholls, J.M., 1973. The Airflow over Mountains. Research 1958–1972. WMO Tech. Note No. 127, Geneva, World Meteorological Organization.

Panin, G.N., Tetzlaff, G., Raabe, A., 1998. Inhomogeneity of the land surface and problems in the parameterization of the surface fluxes in natural conditions. Theor. Appl. Climatol. 60, 163–178.

Paw U.K.T., Shaw, R.H., Maitani, T., 1990. Gravity Waves, Coherent Structures and Plant Canopies. In: Proceedings of the Nineth Symposium on Turbulence and Diffusion, Am. Meteorol. Soc., Boston, MA, pp. 244–246.

Ralph, F.M., Neiman, P.J., Keller, T.L., Levinson, D., Fedor, L., 1997. Observations, simulations, and analysis of non-stationary trapped lee waves. J. Atmos. Sci. 54, 1308–1333.

Sakai, R.K., Fitzjarrald, D.R., Moore, K.E., 2001. Importance of low-frequency contributions to eddy fluxes observed over rough surfaces. J. Appl. Meteorol. 40, 2178–2192.

Schimel, D., Kittel, T., Running, S., Monson, R., Turnipseed, A., Anderson, D., 2002. Carbon sequestration studied in Western US mountains. EOS Trans., Am. Geophy. Union 83, 445.

Stull, R.B., 1988. An Introduction to Boundary Layer Meteorology, Kluwer Academic Publishers, Dordrecht.

Sun, J.L., Lenschow, D.H., Mahrt, L., Crawford, T.L., Davis, K.J., Oncley, S.P., MacPherson, J.I., Wang, Q., Dobosy, R.J., Desjardins, R.L., 1997. Lake induced atmospheric circulations during BOREAS. J. Geophys. Res. 102, 29155–29166.

Sun, J., Desjardins, R., Mahrt, L., MacPherson, I., 1998. Transport of carbon dioxide, water vapor, and ozone by turbulence and local circulations. J. Geophys. Res. 103, 25873–25885.

Sun, J.L., Burns, S.P., Lenschow, D.H., Banta, R., Newsom, R., Coulter, R., Frasier, S., Ince, T., Nappo, C., Cuxart, J., Blumen, W., Lee, X., Hu, X.Z., 2002. Intermittent turbulence associated with a density current passage in the stable boundary layer. Bound-Layer Meteorol. 105, 199–219.

Sun, J., Lenschow, D.H., Burns, S.P., Banta, R.M., Newsom, R.K., Coulter, R., Frasier, S., Ince, T., Nappo, C., Balsley, B.B., Jensen, M., Mahrt, L., Miller, D., Skelly, B., 2004. Atmospheric disturbances that generate intermittent turbulence in nocturnal boundary layers. Bound-Layer Meteorol. 110, 255–279.

Turnipseed, A.A., Blanken, P.D., Anderson, D.E., Monson, R.K., 2002. Surface energy balance above a high-elevation subalpine forest. Agric. For. Meteorol. 110, 177–201.

Turnipseed, A.A., Anderson, D.E., Blanken, P.D., Baugh, W., Monson, R.K., 2003. Airflows and turbulent flux measurements in mountainous terrain, Part 1: canopy and local effects. Agric. For. Meteorol. 119, 1–21.

Vickers, D., Mahrt, L., 1997. Quality control and flux sampling problems for tower and aircraft data. J. Ocean. Atmos. Tech. 14, 512–526.

Vickers, D., Mahrt, L., 2003. The cospectral gap and turbulent flux calculations. J. Ocean. Atmos. Tech. 20, 660–672.

Webb, E.K., Pearman, G.I., Leuning, R., 1980. Correction of flux measurements for density effects due to heat and water vapor transfer. Quart. J. Roy. Meteor. Soc. 106, 85–100.

Wilczak, J.M., Oncley, S.P., Stage, S.A., 2001. Sonic anemometer tilt correction algorithms. Bound. Lay. Meteor. 99, 127–150.